Current Biology 23, 2491–2499, December 16, 2013 ©2013 Elsevier Ltd All rights reserved http://dx.doi.org/10.1016/j.cub.2013.10.054

Article

Aurora B Inhibits MCAK Activity through a Phosphoconformational Switch that Reduces Microtubule Association

Stephanie C. Ems-McClung,[1] Sarah G. Hainline,[2] Jenna Devare,[3] Hailing Zong,[2] Shang Cai,[3] Stephanie K. Carnes,[2] Sidney L. Shaw,[2] and Claire E. Walczak[1,*]

[1]Medical Sciences, Indiana University, Bloomington, IN 47405, USA

[2]Department of Biology, Indiana University, Bloomington, IN 47405, USA

[3]Department of Cellular and Molecular Biochemistry, Indiana University, Bloomington, IN 47405, USA

Summary

Background: Proper spindle assembly and chromosome segregation rely on precise microtubule dynamics, which are governed in part by the kinesin-13 MCAK. MCAK microtubule depolymerization activity is inhibited by Aurora B-dependent phosphorylation, but the mechanism of this inhibition is not understood.

Results: Here, we develop the first Förster resonance energy transfer (FRET)-based biosensor for MCAK and show that MCAK in solution exists in a closed conformation mediated by an interaction between the C-terminal domain (CT) and the neck. Using fluorescence lifetime imaging (FLIM) we show that MCAK bound to microtubule ends is closed relative to MCAK associated with the microtubule lattice. Aurora B phosphorylation at S196 in the neck opens MCAK conformation and diminishes the interaction between the CT and the neck. Using FLIM and TIRF imaging, we find that changes in MCAK conformation are associated with a decrease in MCAK affinity for the microtubule.

Conclusions: Unlike motile kinesins, which are open when doing work, the high-affinity binding state for microtubule-depolymerizing kinesins is in a closed conformation. Phosphorylation switches MCAK conformation, which inhibits its ability to interact with microtubules and reduces its microtubule depolymerization activity. This work shows that the conformational model proposed for regulating kinesin activity is not universal and that microtubule-depolymerizing kinesins utilize a distinct conformational mode to regulate affinity for the microtubule, thus controlling their catalytic efficiency. Furthermore, our work provides a mechanism by which the robust microtubule depolymerization activity of kinesin-13s can be rapidly modulated to control cellular microtubule dynamics.

Introduction

Cells use the microtubule (MT) cytoskeleton, a highly organized dynamic array of polymers, for organelle transport during interphase and for the alignment and segregation of chromosomes during mitosis. MTs within cells have highly regulated dynamics due to the action of both MT-stabilizing and -destabilizing proteins. Of particular interest are members of the kinesin-13 family, which play diverse roles during mitosis, including spindle assembly, error correction, and chromosome segregation (reviewed in [1]). Kinesin-13s are regulated in space and time through phosphorylation and protein-protein interactions. How MCAK phosphorylation affects its subcellular localization has been extensively studied [2–7], but how MCAK phosphorylation affects its catalytic cycle is not understood. For most motile kinesins, their catalytic cycle is regulated to ensure that they only hydrolyze ATP when tightly bound to the MT. MT binding is prevented because the kinesin tail domain folds over, interacts with the motor domain, and inhibits its ATPase activity [8–10]. This creates a conformational model for regulation in which kinesins exist in a closed, autoinhibited state in solution but are activated by cargo binding to allow tight coupling to ATPase activity [11]. This type of conformational regulation has been found for multiple kinesins [12–15] and is becoming widely accepted as the universal model for how kinesin activity is controlled.

MCAK is unique from most other kinesins in that it does not use directed motility to associate with MT ends. MCAK can bind to MT ends directly from solution and with high affinity [16, 17] or by rapid 1D diffusion on the MT lattice [18]. Once at the end, it induces a conformational change in the MT lattice, which causes peeled MT protofilaments, resulting in MT depolymerization [16]. While the MT lattice can stimulate the ATPase activity of MCAK [19], maximal stimulation is achieved by MT ends [17, 20], demonstrating that the MT ends are key to the catalytic mechanism of MCAK. Indeed, the basal ATPase activity of MCAK is very low and is stimulated both by MTs and tubulin dimers [17, 19, 21, 22]. The MCAK catalytic cycle is also distinct from kinesins in that ATP hydrolysis rather than product release is the rate-limiting step [20]. Together, these findings support the idea that the mechanisms of catalytic control for kinesins may not in fact be universally conserved.

In addition to the functional differences between MT-depolymerizing and MT-translocating kinesins, the structural organization of kinesin-13 domains is also distinct. MCAK has a centrally located catalytic domain that contains the conserved kinesin MT and ATP binding domains. The N-terminal domain (NT) is dispensable for in vitro MT depolymerization activity [23, 24] and is necessary for subcellular targeting. The positively charged neck is critical for efficient MT depolymerization activity and for MT end targeting [23–25] by modulating the on rate of MCAK to the MT lattice [26]. Structurally, the distal half of the neck is predicted to form a coiled coil, which is not ordered in the human or mouse structures [27]. S196, the major site of Aurora B phosphoregulation, is located within this predicted coiled coil near a cluster of positive charges. The C-terminal domain (CT) of MCAK contains the dimerization domain [21, 24] and contributes to plus tip tracking, kinetochore binding, and MT lattice association [7, 19, 28]. Deletion of the MCAK CT decreases catalytic efficiency by increasing MT lattice association and reducing tubulin dissociation [26]. With the distinct structural organization and complex roles of each individual domain of MCAK, it is difficult to reconcile how a simple tail inhibition model could act to modulate MCAK activity.

Previous studies showed that the NT and the CT coordinate to regulate MCAK MT depolymerization activity [23], as well as MCAK localization to kinetochores and to plus tips of MTs

*Correspondence: cwalczak@indiana.edu

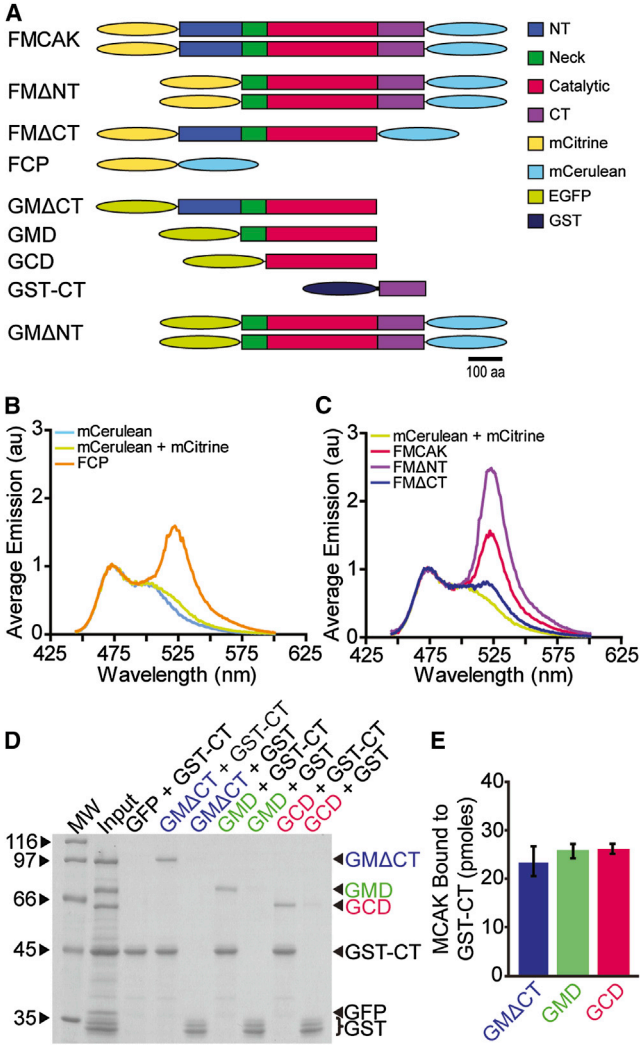

Figure 1. A FRET Reporter Reveals that MCAK Exists in a Closed Conformation in Solution

(A) Primary amino acid structure of FRET reporters: full-length MCAK (FMCAK; dimer), MCAK without the N-terminal domain (NT) (FMΔNT; dimer), MCAK without the C-terminal domain (CT) (FMΔCT; monomer), or FRET positive control protein (FCP). Primary amino acid structure of GFP fusion proteins is as follows: MCAK without the NT (GMΔNT), MCAK without the CT (GMΔCT), MCAK with the neck and catalytic domain (GMD), or the MCAK catalytic domain alone (GCD). The CT fused to GST is also shown (GST-CT). Scale bar represents 100 amino acids.

(B and C) Purified protein was excited at 433 nm, the emission spectra were recorded from 445 to 600 nm, and the average emission spectrum was graphed from three independent experiments.

(D) 10% SDS-PAGE Coomassie-stained gel of the input and bound fractions of a representative glutathione pull-down assay in which GST-CT or GST alone was incubated with control GFP, GMΔCT, GMD, or GCD. MW, molecular weight markers. Input, protein input.

(E) Quantification of three independent pull-down experiments. Average pmol ± SEM of MCAK proteins bound to GST-CT is graphed.

[7, 29]. It was interesting to then speculate that MCAK perhaps uses its nonmotor domains to modulate both its catalytic and physiological activities in cells. Here, we describe the development of the first Förster resonance energy transfer (FRET) biosensor for the kinesin-13 MCAK that detects conformational changes in the MCAK molecule during catalysis. Our studies show that kinesin-13s use a novel conformational regulatory mechanism to tightly control their MT depolymerization activity.

Results

A FRET Reporter Reveals that MCAK Exists in a Closed Conformation in Solution

To test the hypothesis that MCAK MT depolymerization activity might be regulated by conformational changes within the protein, we designed FRET reporters of full-length MCAK (FMCAK) and MCAK with different domain deletions (Figure 1A). Addition of the mCitrine and mCerulean fluorophores did not alter the relative MT depolymerization activities of the proteins (see Figure S1A available online) or the ability of FMCAK to rescue spindle assembly in extracts (Figure S1B) [23]. To analyze the ability of the constructs to exhibit a FRET signal, we excited each of the FRET reporters and recorded their emission spectrum. No FRET signal resulted from mCerulean alone or mCerulean and mCitrine combined (Figure 1B). However, the FRET control protein (FCP, mCitrine fused to mCerulean) displayed positive FRET. FMCAK, FMΔNT, and FMΔCT exhibited varying levels of FRET, with FMΔNT having the highest FRET signal and FMCAK's signal being slightly lower (Figure 1C). This increased FRET emission was not due to excitation of the acceptor, as addition of a molar excess of mCitrine to either FCP or FMCAK did not increase the 525 nm emission (Figure S1C). In addition, the increased FRET emission was not due to intermolecular FRET, because there was no FRET signal when mCit-MCAK was combined with MCAK-mCer (Figure S1D). These results suggest that the NT and neck are in close proximity to the CT and that removal of the CT reduces FRET, showing that the CT is needed for the high FRET conformation. Because high FRET indicates that the NT and CT are in close proximity, whereas low FRET indicates that they are further apart, we define the high FRET conformation as "closed" and the low FRET conformation as "open" to define two distinct conformations of the molecule. However, the structural arrangement of the domains and the magnitude of the differences in conformation between these two states cannot be specifically assessed by this methodology.

The closed conformation of MCAK could be modulated by an interaction between the CT and the NT, neck, or catalytic domain. To test this idea, we performed pull-down experiments in which the MCAK CT was fused to GST (GST-CT) and incubated with GFP-tagged derivatives of MCAK containing variations of the NT, neck, and catalytic domain (Figure 1A) [21, 23]. All three GFP-tagged MCAK deletion proteins were pulled down with GST-CT, whereas the GFP control protein was not (Figures 1D and 1E). These results support the idea that the high FRET MCAK conformation is minimally mediated through a direct interaction between the CT and the catalytic domain.

Aurora B Phosphorylation Induces a Conformational Change in MCAK by Disrupting the Interaction between Domains

Aurora B phosphorylation at S196 in the MCAK neck domain inhibits its MT depolymerization activity and thus could regulate MCAK by changing its conformation. Because MCAK has multiple Aurora B phosphorylation sites in the NT, we chose to use FMΔNT, which eliminates the majority of these sites but retains the key regulatory site at S196 (Figure S2A) [2–4]. We treated FMΔNT with purified Aurora B/INCENP (Aur B) and measured FRET. Aurora B phosphorylation significantly reduced the FRET emission of FMΔNT (Figure 2A) and the

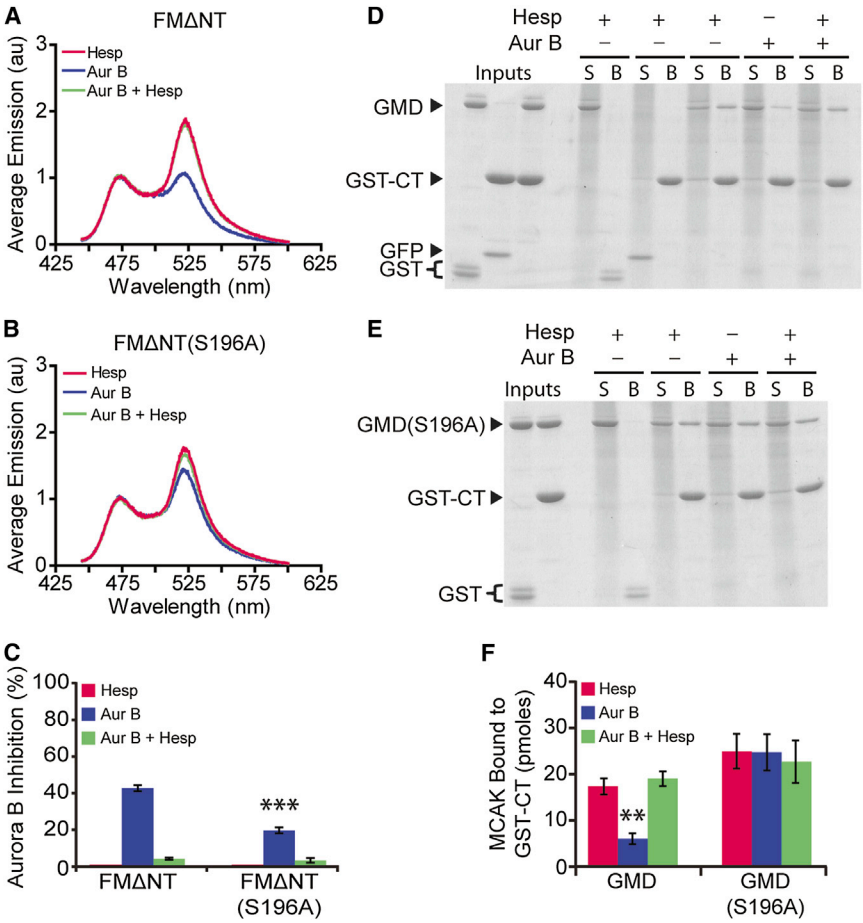

Figure 2. Aurora B Phosphorylation "Opens" MCAK by Inhibiting the Interaction between the Neck and the CT

(A) FMΔNT was treated with hesperadin (Hesp), Aurora B/INCENP (Aur B), or both Aurora B and hesperadin and excited at 433 nm, and the emission spectra were recorded and graphed as the average of three independent experiments.

(B) Emission spectra of FMΔNT(S196A) treated with the indicated conditions and graphed as in (A).

(C) Quantification of the percent inhibition of the FRET ratio from three independent experiments. The mean ± SEM is graphed. ***$p < 0.001$.

(D) 10% SDS-PAGE Coomassie-stained gel of the input, supernatant (S), and bound (B) fractions of a representative glutathione pull-down assay with GMD ± hesperadin and Aurora B/INCENP.

(E) 10% SDS-PAGE Coomassie-stained gel of a representative glutathione pull-down assay with GMD(S196A) as in (D).

(F) Quantification of four independent pull-down experiments. Average pmol of GMD or GMD(S196A) bound to GST-CT ± SEM is graphed. **$p < 0.01$.

FRET ratio of FMCAK and FMΔCT but had no effect on FCP (Figure S2B). Inhibition required Aurora B catalytic activity, because inclusion of the Aurora B inhibitor hesperadin in the phosphorylation reaction blocked the changes in FRET (Figure 2A; Figure S2B). Aurora B-dependent inhibition of FRET was also significantly diminished in FMΔNT(S196A) (Figures 2B and 2C), suggesting that this site is required for the conformational change.

To determine whether MCAK phosphorylation also disrupts the interaction between MCAK domains, we repeated the pull-down experiments with Aurora B-phosphorylated MCAK truncation proteins. Aurora B phosphorylation significantly reduced the binding of GST-CT to GMD (Figure 2D; Figure S2C), which was prevented by inclusion of hesperadin in the reaction, showing that reduced binding required Aurora B catalytic activity (Figures 2D and 2F; Figures S2C and S2D). In contrast, Aurora B did not affect the binding of GST-CT to GMD(S196A) (Figures 2E and 2F) or GCD (Figures S2C and S2D), demonstrating that phosphorylation of S196 within the neck is critical for this interaction. Together, our data support the model that Aurora B regulates MCAK activity by disrupting an interaction between the catalytic domain and the CT that is dependent on the neck, and this regulation correlates with a conformational change in MCAK.

MCAK Binds MT Ends in a More "Closed" Conformation Relative to the Lattice

If MCAK activity is regulated by conformational changes, then MCAK conformation should change upon binding to its substrates and may bind MT ends and lattice differentially. To test this idea, we developed a plate-based assay in which we calculated the FRET ratio of fluorescence intensity (I_F/I_D) at the peak emission wavelengths of the acceptor (I_F) and the donor (I_D) fluorophores (Figure S2B) in the presence of increasing concentrations of MTs. We found a MT concentration-dependent decrease in FMCAK FRET ratio ($p < 0.001$), in contrast to the control proteins that showed no dose-dependent effect (Figure 3A). Because the MCAK catalytic cycle model predicts that MCAK dissociates from tubulin dimers at the end of its catalytic cycle, we also asked whether tubulin dimers affected MCAK conformation. Similar to that seen with MTs, increasing concentrations of tubulin dimers caused a decrease in the FRET ratio ($p < 0.001$) (Figure 3B), indicating that MCAK binding to free tubulin dimers also causes conformational changes in MCAK.

The above results are consistent with the idea that MCAK changes conformation during its catalytic cycle, but they do not indicate where on the MT these changes occur. To address this more directly, we utilized fluorescence lifetime imaging (FLIM) to measure the corresponding mCerulean lifetimes of FMCAK bound to MTs (Table S1). If FRET occurs, the lifetime will shift to smaller values due to energy transfer from the donor to acceptor. When bound to MTs, FMCAK had a smaller lifetime (1.76 ns) relative to control MCAK-mCer (2.00 ns, $p < 0.0001$) (Figures 3C and 3E). There was no difference in the lifetime of MCAK-mCer at the ends (1.99 ns) versus the lattice (2.01 ns, $p = 0.12$) (Figure 3D). In contrast, FMCAK had a shorter lifetime at the ends (1.73 ns) relative to the lattice (1.78 ns, $p < 0.0001$) (Figure 3E), consistent with the idea that MCAK bound to the MT ends is in a more "closed" conformation relative to MCAK bound to the MT lattice.

To rule out the possibility that intermolecular interactions occur at MT ends due to the enrichment of MCAK, we carried out FLIM imaging of mCit-MCAK combined with MCAK-mCer. The lifetime of mCit-MCAK + MCAK-mCer on MTs (1.90 ns)

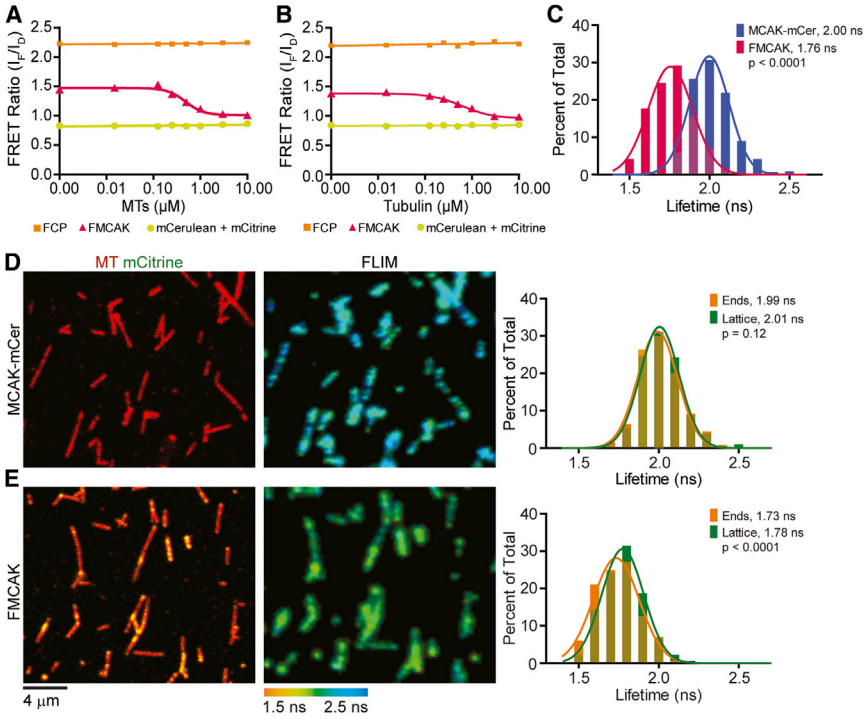

Figure 3. MCAK Binds Microtubule Ends in a Closed Conformation Relative to the Microtubule Lattice

(A and B) Average I_F/I_D ratio of mCerulean + mCitrine, FCP, or FMCAK with increasing concentrations of GMPCPP/paclitaxel-stabilized microtubules (MTs) (A) or GDP-tubulin dimers (B) from three independent experiments. The best-fit linear regression line was modeled through the mCerulean + mCitrine and FCP data points, and the best-fit four-parameter dose-response curve was modeled through the FMCAK data points. The average ± SEM is graphed for each data point.

(C) Quantification of fluorescence lifetimes of either control MCAK-mCer or FMCAK bound to MTs. Histograms represent quantification of at least 50 MTs in four or five independent experiments. The mean fluorescence lifetime calculated from the Gaussian distribution is indicated with the associated p value for the difference in lifetime distributions.

(D) Corresponding confocal (left) and FLIM (middle) images of MCAK-mCer bound to MTs. Right: quantification of MCAK-mCer spots for MT end or lattice fluorescence lifetimes.

(E) Corresponding confocal (left) and FLIM (middle) images of FMCAK bound to MTs. Right: quantification of FMCAK spots for MT end or lattice fluorescence lifetimes.

was indistinguishable from MCAK-mCer alone (1.91 ns, p = 0.47) but was significantly higher than that of FMCAK (1.76 ns, p < 0.0001) (Figures S3A and S3B). There was a slight decrease in the lifetime of mCit-MCAK + MCAK-mCer at MT ends (1.88 ns) versus the MT lattice (1.92 ns, p < 0.0001) (Figure S3C), but these lifetimes were still significantly higher than that of FMCAK at MT ends (1.74 ns, p < 0.0001). As a further control to demonstrate that the reduced lifetimes were not due to clusters of MCAK on the MT, we found no correlation between the lifetimes and the corresponding mCerulean photon counts (Figures S3E), suggesting that the changes in lifetime of FMCAK at MT ends represent MCAK being in a more "closed" conformation.

Aurora B Phosphorylation Opens the Conformation of MCAK on MT Ends and Lattice and Reduces Its Binding to the MT

Because Aurora B phosphorylation caused MCAK to shift conformation in solution, we asked how phosphorylation affected MCAK on the MT. Aurora B phosphorylation had no effect on the overall lifetime of control MCAK-mCer (2.02 ns, p = 0.070), nor were there any differences in lifetime of MCAK-mCer at the MT ends (2.01 ns) or lattice (2.03 ns, p = 0.14) (Figures 4A and 4B; Table S1). In contrast, phosphorylation of MCAK by Aurora B caused a higher overall lifetime of FMCAK on MTs (1.86 ns, p < 0.0001) (Figures 4C and 4D). Phosphorylated MCAK had higher lifetimes on both the ends (1.83 ns) and the lattice (1.89 ns) relative to nonphosphorylated MCAK, which were statistically different from each other (p < 0.001). FMCAK(S196A) displayed a smaller lifetime than FMCAK (1.64 ns, p < 0.0001) and had smaller lifetimes at MT ends (1.69 ns) relative to the lattice (1.71 ns, p < 0.0001), consistent with the differences we see with FMCAK. The smaller lifetime of FMCAK(S196A) relative to FMCAK is consistent with our previous finding that MCAK is partially phosphorylated upon purification from insect cells [3].

If Aurora B inhibits MCAK MT depolymerization activity through S196 by conformational regulation, then we would expect the S196A mutation to abrogate the Aurora B reduction in FRET not only in solution but also on the MT by FLIM. Indeed, FMCAK(S196A) had a smaller change in lifetime upon Aurora B phosphorylation compared to FMCAK, consistent with the change in solution (Figures 4E and 4F). The difference in lifetime of nonphosphorylated (1.64 ns) and phosphorylated FMCAK(S196A) (1.70 ns) was statistically significant (p < 0.0001), consistent with the idea that Aurora B is also modulating the conformation of MCAK through other sites or mechanisms.

When analyzing the FLIM images, we noticed that Aurora B phosphorylation caused a significant reduction in FMCAK bound to the MT (Figure 4C). To measure this effect, we used a custom-built MATLAB algorithm to quantify FMCAK bound to the MTs in the absence or presence of Aurora B (Figures S3F and S3G). We found that Aurora B phosphorylation reduced the percentage of MTs with FMCAK bound (p < 0.01), which was dependent on S196 phosphorylation. Of the MTs with bound MCAK, Aurora B phosphorylation reduced both FMCAK and FMCAK(S196A) binding to the lattice (p < 0.01), but there was no effect on the ends. This indicates that S196 is not the only site that contributes to this effect. We also used bulk sedimentation assays to show that the amount of FMCAK bound to MTs at saturating MT concentrations was reduced with Aurora B phosphorylation (Figures S3H and S3I). Together, these results show that MCAK binds MT ends in a more "closed" conformation relative to the lattice and that phosphorylated MCAK cannot bind to the MT lattice as well and maintains a more "open" conformation when bound to the MT.

Aurora B Phosphorylation Increases the 1D Diffusion and Off Rate of MCAK from the MT

The dramatic reduction in MCAK binding upon phosphorylation indicates defects in MT affinity. Previous studies showed

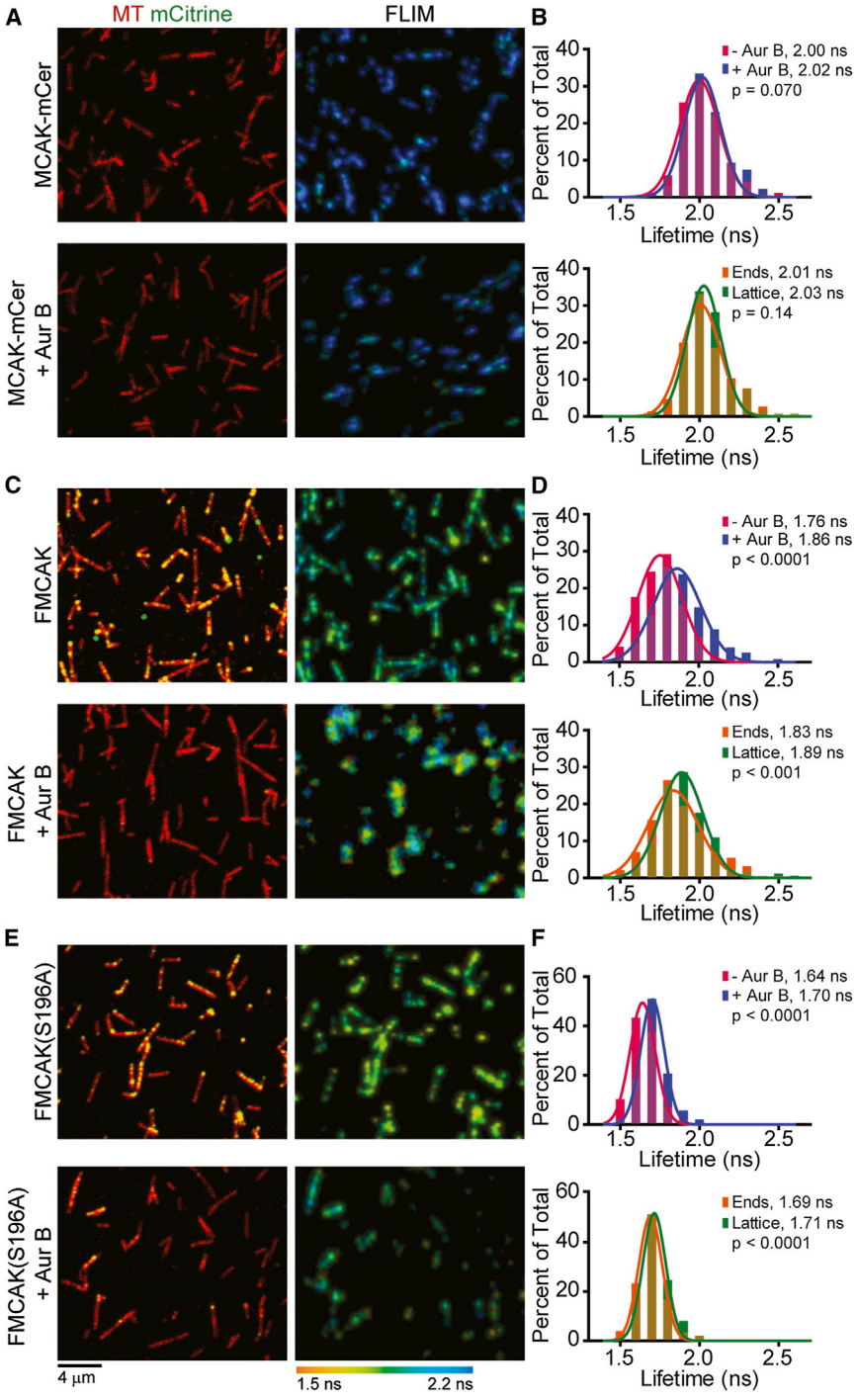

Figure 4. Aurora B Phosphorylation Opens MCAK Conformation when Bound to MTs

(A) Corresponding confocal (left) and FLIM (right) images of control MCAK-mCer bound to MTs in the absence (top) or presence (bottom) of Aurora B.

(B) Quantification of MCAK-mCer fluorescence lifetimes from three independent experiments in which at least 50 MTs were quantified per experiment. The mean fluorescence lifetime calculated from the Gaussian distribution is indicated with the associated p value for the difference between lifetime distributions. Top: distributions of lifetimes of MT-bound MCAK-mCer in the absence (red) or presence of Aurora B (blue). Bottom: distributions of lifetimes at the MT ends (orange) or lattice (green) in the presence of Aurora B.

(C) Corresponding confocal (left) and FLIM (right) images of FMCAK bound to MTs in the absence (top) or presence (bottom) of Aurora B.

(D) Quantification of fluorescence lifetimes from five independent experiments in which at least 50 MTs were quantified per experiment. Top: distributions of lifetimes of MT-bound FMCAK in the absence (red) or presence of Aurora B (blue). Bottom: distributions of lifetimes at the MT ends (orange) or lattice (green) in the presence of Aurora B.

(E) Corresponding confocal (left) and FLIM (right) images of FMCAK(S196A) bound to MTs in the absence (top) or presence (bottom) of Aurora B.

(F) Quantification of fluorescence lifetimes from three independent experiments in which at least 50 MTs were quantified per experiment. Top: distributions of lifetimes of MT-bound FMCAK(S196A) in the absence (red) or presence (blue) of Aurora B. Bottom: distributions of lifetimes at the MT ends (orange) or lattice (green) in the presence of Aurora B.

Note that the control data sets (−Aur B) for both MCAK-mCer and FMCAK are the same data sets used for the analysis of Figure 3. Number of spots can be found in Table S1.

that MCAK on rate to the MT is facilitated by the charged residues in the neck and is key for efficient flux to the MT end [26]. Thus, we hypothesized that phosphorylation in the neck might affect the on rate of MCAK by neutralizing the positive charge in the neck. To test this idea, we performed single-molecule total internal reflection fluorescence (TIRF) microscopy of nonphosphorylated and phosphorylated GFP-tagged MCAK containing aa 187–730 (GMΔNT). We used this construct because only the S196 site that regulates MT depolymerization activity is retained in this region (Figure 5). Two-step bleaching analyses showed that single dimers of GMΔNT were imaged (Figure S4A). Furthermore, the intensity distribution of the molecules did not change with the addition of Aurora B (Figures S4B and S4C), supporting the idea that Aurora B does not simply prevent clustering of MCAK molecules on MTs. Surprisingly, there were no differences in the on rates between ends and lattice, and phosphorylation had no effect on the on rates (Table S2). MCAK mean square displacement analysis on the lattice and ends showed that there is very little if any 1D diffusion on the MT ends independent of condition, which might be expected for the constrained location of the MT end and could be indicative of a specific conformation of MCAK (Figures 5B and 5E). 1D diffusion on the lattice was dramatically higher than on the MT ends for all conditions. While neutralization of the neck by amino acid substitution did not affect the 1D diffusion of MCAK [26], Aurora B phosphorylation of GMΔNT increased the 1D diffusion on the lattice by 1.7-fold, but not the 1D diffusion of GMΔNT(S196A) (Figures S5A and S5B). This suggests that

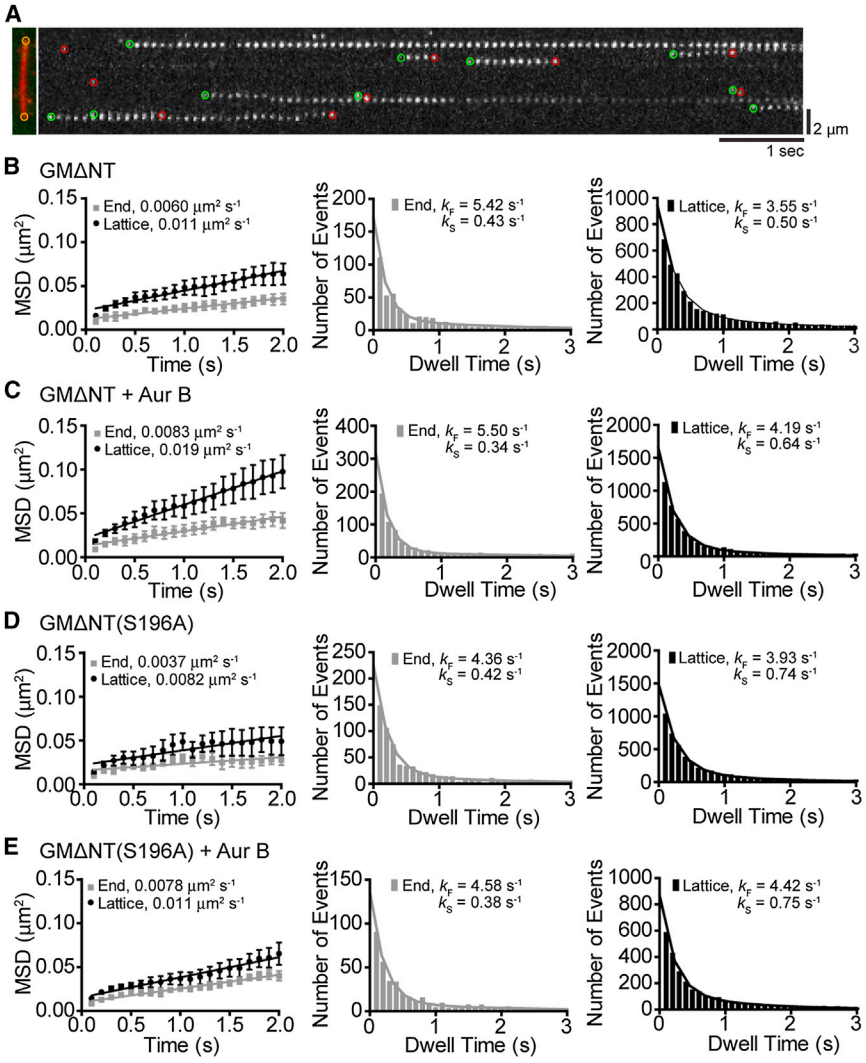

Figure 5. Aurora B Phosphorylation Increases the 1D Diffusion and the Off Rate of MCAK from the MT

(A) Fluorescence micrograph overlay (left) of GMΔNT (green) on a MT (red) and 9 s of the corresponding 60 s kymograph generated from that data (right). MTs were identified from an overlay of the MTs on the GMΔNT movie by drawing a segmented line through the MT (not shown) followed by marking of the MT ends (yellow circles). Events were identified manually by placing a dot (green circle) on the first appearance of GMΔNT and a dot (red circle) on the last frame of the event. This allowed the identification of events that were within one to two pixels of one another. Single-frame events resulted in the placement of start and stop dots on top of one another. Note that because this is a partial kymograph, three spots persisted beyond this image and are not marked with a red circle.

(B–E) TIRF imaging of GMΔNT (B and C) or GMΔNT(S196A) (D and E) in the absence (B and D) or presence (C and E) of Aurora B/INCENP (Aur B). Mean square displacements ± SEM (left) for the MT ends (gray) and the lattice (black) were calculated from the analysis of thousands of events per condition and plotted versus the lag time. A linear regression was fit to the data without constraining the y intercept to zero. Diffusion coefficients were determined from the slope of the linear regression divided by two and are indicated. The dwell-time histograms from MT end events (middle, gray) and lattice events (right, black) are graphed with the best-fit two-phase exponential decay curve from which the corresponding fast (k_F) and slow (k_S) dissociation rates are indicated.

the more "open" conformation induced by Aurora B phosphorylation at S196 may result in a looser association to the MT lattice.

Because the MCAK on rate to the MT was not affected by phosphorylation, there could be an increase in the MT off rate of phosphorylated MCAK to account for the decreased binding in the FLIM and MT pelleting assays. Interestingly, the dwell times of MCAK on the MT ends and lattice fit a two-phase exponential decay better than a one-phase as assessed by residual plots and nonlinear plots of the transformed data (Figures 5B–5E; Figures S5C–S5H). This illustrates that there are two populations of binding events on both the lattice and the ends with distinct off rates. For MT ends, the slow off rate (k_S) of GMΔNT was not statistically different from GMΔNT with Aurora B, GMΔNT(S196A), or GMΔNT(S196A) with Aurora B, indicating that this population is not affected by Aurora B phosphorylation (Figures 5B–5E; Table S2). Similarly, the fast off rates (k_F) of GMΔNT and GMΔNT(S196A) were not statistically different from the fast off rates with Aurora B. These findings are consistent with the FLIM binding analysis in which Aurora B phosphorylation did not affect FMCAK binding to MT ends.

For the MT lattice, Aurora B phosphorylation of GMΔNT increased the slow off rate 1.3-fold relative to nonphosphorylated GMΔNT ($p < 0.001$) (Figures 5B and 5C; Table S2). In contrast, phosphorylation of GMΔNT(S196A) did not change the slow off rate ($p = 0.79$), consistent with an S196-dependent mechanism (Figures 5D and 5E; Table S2). Aurora B phosphorylation increased the fast off rate of both GMΔNT and GMΔNT(S196A) ($p < 0.0001$), suggesting an S196-independent mechanism. These results are consistent with our FLIM MT binding analysis where we saw both S196-dependent and -independent mechanisms.

Aurora B Phosphorylation Reduces the Affinity of MCAK for Tubulin Dimers

The final part of the MCAK catalytic cycle requires that MCAK be dissociated from tubulin dimers. One possibility is that phosphorylated MCAK could have an increased affinity for tubulin dimers, which would slow the recycling step and reduce the overall amount of MT depolymerization. Alternatively, phosphorylated MCAK might have a decreased affinity for tubulin dimers, indicative of its reduced binding to MTs seen in the FLIM and TIRF imaging. We used microscale thermophoresis to measure the K_d of the interaction between GMΔNT and tubulin with or without Aurora B (Figure 6). We found a 16-fold increase in the K_d of Aurora B-phosphorylated GMΔNT for tubulin dimers relative to nonphosphorylated GMΔNT, consistent with the idea that Aurora B phosphorylation reduces the overall affinity of MCAK for its substrates by changing its conformation.

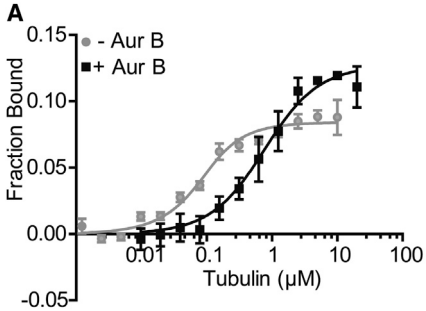

B

	K_d(μM)	Percent Bound (%)
GMΔNT	0.044	8.4
(95% CI)	(0.022 to 0.066)	(7.9 to 8.9)
GMΔNT + Aur B	0.70	13
(95% CI)	(0.38 to 1.00)	(11 to 14)

Figure 6. Aurora B Phosphorylation Inhibits the Affinity of MCAK for Tubulin Dimers

(A) Binding curve of the fraction of GMCAK bound to tubulin dimers in the absence (gray) or presence (black) of Aurora B kinase. The means ± SEM from at least three independent experiments is plotted and fit to the best-fit quadratic binding curve.

(B) Summary of the data derived from the graphs in (A). CI, confidence interval.

Discussion

Here we have developed the first biosensor for the nonconventional kinesin family member MCAK. We detected conformational changes between the MCAK CT and neck domains, which are controlled by Aurora B phosphorylation. Evidence is mounting that conformational changes are an effective way to modulate kinesin activity [11]. Most kinesins exist in a closed state in solution [8, 14, 30], in which the tail folds back and inhibits MT-stimulated ATPase activity [8–10]. This autoinhibition is postulated to ensure that kinesins are only active for motility when bound to cargo. Previous studies suggest that MCAK might also undergo some type of conformational regulation to regulate its activities [23]. Structural studies support this idea because in the crystal structure, the orientation of the neck is either angled down perpendicular to the longitudinal axis of the MT within close proximity to where the CT extends from the catalytic domain (Figures S6A and S6B) or points back toward the minus end at a significant distance from where the CT exits the catalytic domain (Figure S6C), consistent with this domain being flexible [27]. The absence of the CT in these crystallized proteins could contribute to the observed flexibility of the neck, if interaction with the negatively charged CT regions stabilizes the orientation of the positively charged neck (Figure S6D). Consistent with this model, deletion or neutralization of the positive charges within the predicted neck coiled coil disrupts MCAK MT depolymerization activity [24, 25]. From our work, we propose that the CT interacts tightly with the neck and that this interaction is regulated by Aurora B phosphorylation, which serves as a critical mediator of MCAK activity.

MCAK catalytic activity is distinct from that of other kinesins. For most kinesins, product release is the rate-limiting step for ATP turnover [31]. For MCAK, ATP cleavage is the rate-limiting step, and MCAK is predominantly ATP bound in solution [20]. MCAK ATPase activity is stimulated by the MT lattice [19–21, 32], but its ATPase activity is maximally activated by MT ends where it achieves a tightly bound state needed for MT depolymerization [17, 20]. Wagenbach et al. have proposed that there are two transition states that MCAK goes through for MT depolymerization prior to ATP hydrolysis: high-affinity end binding and tubulin detachment from the MT [33]. The MCAK conformational changes that we show in this study likely correlate with these different nucleotide and MT binding states (Figure 7A). We propose that in solution, MCAK is ATP bound and in a "closed" conformation. Binding to the MT lattice correlates with a conformational change that "opens" MCAK relative to MCAK in solution, and this "open" conformation would be the posthydrolysis ADP-Pi state that is competent for 1D diffusion. This idea is consistent with the finding that MCAK has lattice-stimulated ATPase activity [19], with our results showing that increasing amounts of MTs decrease the FRET ratio, and that MCAK has a larger fluorescence lifetime when bound to the lattice relative to the MT end. Upon reaching the MT end, there is rapid exchange of ADP for ATP [20], which forms the high-affinity prehydrolysis end-binding state that detaches a tubulin dimer from the MT. Our data showing that MCAK at the MT end is more "closed" relative to MCAK bound to the MT lattice are consistent with the idea that ATP-bound MCAK forms the high-affinity end-binding state, which is in a "closed" conformation. This argues that unlike conventional kinesin, the active MCAK conformation is "closed" rather than "open." Upon release of the MCAK-tubulin complex from the MT, ATP is hydrolyzed, concomitant with an additional MCAK conformational change to a more "open" conformation, supporting the idea that conformational changes are coordinated with the MCAK catalytic cycle. MCAK is then recycled upon dissociation from tubulin dimers, which is associated with a change to the "closed" conformation. This mechanism would also explain why the CT is necessary for efficient recycling, because it plays an important role in the conformational changes of MCAK.

This proposed mechanism also explains how the observed changes in conformation mediated by Aurora B phosphorylation would be effective in modulating MCAK catalytic activity (Figure 7B). Aurora B phosphorylation converts MCAK from a "closed" to "open" conformation. Because MCAK associated with the lattice is normally "open," phosphorylated MCAK might be expected to have higher 1D diffusion. Indeed, we found that phosphorylated MCAK has increased 1D diffusion relative to nonphosphorylated MCAK and is dependent on S196 phosphorylation. However, by shifting MCAK to this "open" conformation, we speculate that phosphorylation prevents MCAK from forming the high-affinity "closed" state at MT ends, which is the key active conformation for inducing MT depolymerization. This idea is consistent with our finding that Aurora B phosphorylation increases the fluorescence lifetime of MCAK on MT ends in addition to the lattice. The finding that the affinity for tubulin dimers is significantly reduced when MCAK is phosphorylated suggests that the conversion from an "open" to a "closed" state must occur after release of MCAK from tubulin dimers, which is when ATP exchange occurs in solution. Thus, unlike conventional kinesin, which goes from a closed, autoinhibited state in solution to an open, active state when transporting cargo, MCAK must go through multiple conformations within a single catalytic cycle. Thus, the MCAK conformational cycle is uniquely tuned to ensure that MCAK is an effective MT depolymerase. This illustrates a novel

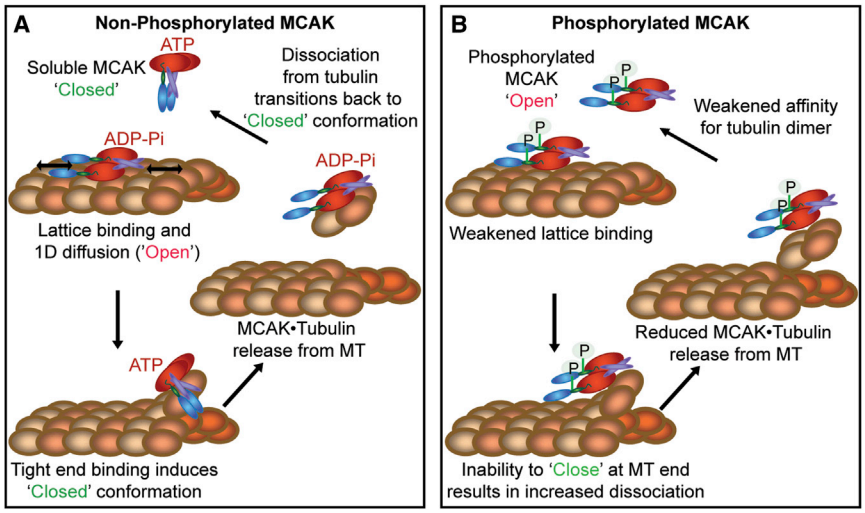

Figure 7. Model for How the Aurora B-Induced Phosphoconformational Switch Regulates MCAK Activity

(A) In solution, ATP-bound MCAK is in a closed state. Upon binding the MT lattice, ATP is rapidly hydrolyzed, which is associated with an MCAK conformational change to the open state. MT end binding stimulates MCAK nucleotide exchange and shifts MCAK into the closed high-affinity MT end conformation. MCAK is released from the MT end in a complex with tubulin dimers, where a second round of ATP hydrolysis occurs, shifting MCAK to a more open conformation, which has a reduced affinity for tubulin dimers, thereby facilitating release of the tubulin dimers and recycling of the MCAK for another round of MT depolymerization.

(B) Phosphorylation of MCAK switches it to an open conformation. Phosphorylated MCAK is still competent to bind the MT lattice, but with reduced affinity, and exhibits increased 1D diffusion. Phosphorylated MCAK cannot achieve the high-affinity MT end binding conformation and thus more rapidly dissociates from the MT end, inhibiting MT depolymerization. Any phosphorylated MCAK molecules in association with tubulin dimers are rapidly released due to its lowered affinity for tubulin dimers.

mechanism by which conformation can regulate the activity of kinesin family members.

We also found a modest effect of Aurora B phosphorylation on MCAK MT lattice 1D diffusion. Previous studies have reported widely different values for the 1D diffusion rates [18, 26] in which our values are more consistent with those of Cooper et al. [26], who used similar ionic strength buffers and tubulin source. Our reported values for 1D diffusion and those of Cooper et al. [26] are likely too low to account for a physiological important mechanism by which MCAK reaches the MT end. Instead, we favor the idea that the Aurora B-induced increase in 1D diffusion represents the ability of conformational changes in MCAK to regulate its MT affinity.

MCAK is a potent MT depolymerase and therefore requires a mechanism to restrain its activity in cells. The differential regulation of MCAK conformation relative to that of other kinesins may be specifically adapted for the fine-tuned regulation that MCAK must undergo to precisely control MT dynamics under very rapid timescales. It is perhaps surprising that Aurora B effects on MCAK MT behavior were modest in magnitude, but we should consider how Aurora B modulates kinetochore-MT interactions. MCAK is important for preventing or correcting improper kinetochore-MT attachments [34], and it was attractive to speculate that MCAK might be the major Aurora B downstream target in error correction [2, 3, 35]. However, inhibition of MCAK only moderately affects the stabilization of K fiber MT dynamics [36, 37] relative to the very large stabilization caused by inhibiting Aurora B [38] and has no effect on the correction of syntelic attachments during mitosis [39]. It is more likely that Aurora B acts through the Ndc80 complex to facilitate MT detachment for error correction [40, 41] and uses MCAK to strengthen or weaken these attachments to modulate the system. This is consistent with MCAK facilitating chromosome movement by weakening kinetochore attachments, which may indirectly aid in error correction by changing the MT attachment status within a K fiber bundle [37].

Aurora B additionally regulates MCAK by controlling its subcellular targeting. Phosphorylation is required to target MCAK to kinetochores, where Aurora B modulates MCAK turnover kinetics [2, 3, 35]. The NT of MCAK, which contains many of the Aurora B phosphorylation sites, is sufficient for kinetochore targeting [42], but both the NT and the CT are needed for efficient localization [23, 28, 35], suggesting that conformational regulation may also play an important role in subcellular targeting. We propose that kinesin-13s target to their respective cellular locations in the "closed" state, wherein they are locally regulated through phosphorylation or protein-protein interactions that may alter conformation. Together, these studies suggest that MCAK conformation may act like a rheostat to finely tune its activity and to provide a mechanism to adjust rapidly to cellular needs for changing MT dynamics. An important future direction will be to take advantage of these FRET reporters to understand the conformational state of MCAK at distinct locales and to measure the dynamic changes in MCAK conformation that are associated with its regulated activity.

Supplemental Information

Supplemental Information includes six figures, two tables, and Supplemental Experimental Procedures and can be found with this article online at http://dx.doi.org/10.1016/j.cub.2013.10.054.

Acknowledgments

This work was supported by NIH grant GM 059618 to C.E.W., NSF grant MCB 1157982 to S.L.S., and Hutton Honors College Summer Research Fellowships to J.D. and S.K.C. The IU Light Microscopy Imaging Center is supported in part by the Office of the Vice Provost for Research at IU. We thank Todd Stone, Jim Powers, Irina Tsvetkova, Riyaz Bhat, Ana Lazic, Kirsten Verhey, Tarun Kapoor, Xin Zhang, Joan Walker, Joel Ybe, Rik Van Gorsel, and Rich Day for discussions and technical assistance. We thank Bogden Dragnea for use of his TIRF microscope. Amanda Rollins assisted in insect cell culture and protein expression, and David Hsieh assisted in the design and optimization of some of the MATLAB code. We thank Linda Wordeman for sharing original movie data. Jared Cochran and Lesley Weaver provided comments on the manuscript.

Received: July 2, 2013
Revised: September 12, 2013
Accepted: October 21, 2013
Published: November 27, 2013

References

1. Walczak, C.E., Gayek, S., and Ohi, R. (2013). Microtubule-depolymerizing kinesins. Annu. Rev. Cell Dev. Biol. *29*, 417–441.

2. Andrews, P.D., Ovechkina, Y., Morrice, N., Wagenbach, M., Duncan, K., Wordeman, L., and Swedlow, J.R. (2004). Aurora B regulates MCAK at the mitotic centromere. Dev. Cell *6*, 253–268.
3. Lan, W., Zhang, X., Kline-Smith, S.L., Rosasco, S.E., Barrett-Wilt, G.A., Shabanowitz, J., Hunt, D.F., Walczak, C.E., and Stukenberg, P.T. (2004). Aurora B phosphorylates centromeric MCAK and regulates its localization and microtubule depolymerization activity. Curr. Biol. *14*, 273–286.
4. Ohi, R., Sapra, T., Howard, J., and Mitchison, T.J. (2004). Differentiation of cytoplasmic and meiotic spindle assembly MCAK functions by Aurora B-dependent phosphorylation. Mol. Biol. Cell *15*, 2895–2906.
5. Zhang, X., Ems-McClung, S.C., and Walczak, C.E. (2008). Aurora A phosphorylates MCAK to control ran-dependent spindle bipolarity. Mol. Biol. Cell *19*, 2752–2765.
6. Jiang, K., Wang, J., Liu, J., Ward, T., Wordeman, L., Davidson, A., Wang, F., and Yao, X. (2009). TIP150 interacts with and targets MCAK at the microtubule plus ends. EMBO Rep. *10*, 857–865.
7. Moore, A.T., Rankin, K.E., von Dassow, G., Peris, L., Wagenbach, M., Ovechkina, Y., Andrieux, A., Job, D., and Wordeman, L. (2005). MCAK associates with the tips of polymerizing microtubules. J. Cell Biol. *169*, 391–397.
8. Friedman, D.S., and Vale, R.D. (1999). Single-molecule analysis of kinesin motility reveals regulation by the cargo-binding tail domain. Nat. Cell Biol. *1*, 293–297.
9. Hackney, D.D., and Stock, M.F. (2000). Kinesin's IAK tail domain inhibits initial microtubule-stimulated ADP release. Nat. Cell Biol. *2*, 257–260.
10. Imanishi, M., Endres, N.F., Gennerich, A., and Vale, R.D. (2006). Autoinhibition regulates the motility of the C. elegans intraflagellar transport motor OSM-3. J. Cell Biol. *174*, 931–937.
11. Verhey, K.J., and Hammond, J.W. (2009). Traffic control: regulation of kinesin motors. Nat. Rev. Mol. Cell Biol. *10*, 765–777.
12. Cai, D., Hoppe, A.D., Swanson, J.A., and Verhey, K.J. (2007). Kinesin-1 structural organization and conformational changes revealed by FRET stoichiometry in live cells. J. Cell Biol. *176*, 51–63.
13. Hammond, J.W., Blasius, T.L., Soppina, V., Cai, D., and Verhey, K.J. (2010). Autoinhibition of the kinesin-2 motor KIF17 via dual intramolecular mechanisms. J. Cell Biol. *189*, 1013–1025.
14. Wedaman, K.P., Meyer, D.W., Rashid, D.J., Cole, D.G., and Scholey, J.M. (1996). Sequence and submolecular localization of the 115-kD accessory subunit of the heterotrimeric kinesin-II (KRP85/95) complex. J. Cell Biol. *132*, 371–380.
15. Espeut, J., Gaussen, A., Bieling, P., Morin, V., Prieto, S., Fesquet, D., Surrey, T., and Abrieu, A. (2008). Phosphorylation relieves autoinhibition of the kinetochore motor Cenp-E. Mol. Cell *29*, 637–643.
16. Desai, A., Verma, S., Mitchison, T.J., and Walczak, C.E. (1999). Kin I kinesins are microtubule-destabilizing enzymes. Cell *96*, 69–78.
17. Hunter, A.W., Caplow, M., Coy, D.L., Hancock, W.O., Diez, S., Wordeman, L., and Howard, J. (2003). The kinesin-related protein MCAK is a microtubule depolymerase that forms an ATP-hydrolyzing complex at microtubule ends. Mol. Cell *11*, 445–457.
18. Helenius, J., Brouhard, G., Kalaidzidis, Y., Diez, S., and Howard, J. (2006). The depolymerizing kinesin MCAK uses lattice diffusion to rapidly target microtubule ends. Nature *441*, 115–119.
19. Moore, A., and Wordeman, L. (2004). C-terminus of mitotic centromere-associated kinesin (MCAK) inhibits its lattice-stimulated ATPase activity. Biochem. J. *383*, 227–235.
20. Friel, C.T., and Howard, J. (2011). The kinesin-13 MCAK has an unconventional ATPase cycle adapted for microtubule depolymerization. EMBO J. *30*, 3928–3939.
21. Hertzer, K.M., Ems-McClung, S.C., Kline-Smith, S.L., Lipkin, T.G., Gilbert, S.P., and Walczak, C.E. (2006). Full-length dimeric MCAK is a more efficient microtubule depolymerase than minimal domain monomeric MCAK. Mol. Biol. Cell *17*, 700–710.
22. Moores, C.A., Yu, M., Guo, J., Beraud, C., Sakowicz, R., and Milligan, R.A. (2002). A mechanism for microtubule depolymerization by KinI kinesins. Mol. Cell *9*, 903–909.
23. Ems-McClung, S.C., Hertzer, K.M., Zhang, X., Miller, M.W., and Walczak, C.E. (2007). The interplay of the N- and C-terminal domains of MCAK control microtubule depolymerization activity and spindle assembly. Mol. Biol. Cell *18*, 282–294.
24. Maney, T., Wagenbach, M., and Wordeman, L. (2001). Molecular dissection of the microtubule depolymerizing activity of mitotic centromere-associated kinesin. J. Biol. Chem. *276*, 34753–34758.
25. Ovechkina, Y., Wagenbach, M., and Wordeman, L. (2002). K-loop insertion restores microtubule depolymerizing activity of a "neckless" MCAK mutant. J. Cell Biol. *159*, 557–562.
26. Cooper, J.R., Wagenbach, M., Asbury, C.L., and Wordeman, L. (2010). Catalysis of the microtubule on-rate is the major parameter regulating the depolymerase activity of MCAK. Nat. Struct. Mol. Biol. *17*, 77–82.
27. Ogawa, T., Nitta, R., Okada, Y., and Hirokawa, N. (2004). A common mechanism for microtubule destabilizers-M type kinesins stabilize curling of the protofilament using the class-specific neck and loops. Cell *116*, 591–602.
28. Maney, T., Hunter, A.W., Wagenbach, M., and Wordeman, L. (1998). Mitotic centromere-associated kinesin is important for anaphase chromosome segregation. J. Cell Biol. *142*, 787–801.
29. Wordeman, L., Wagenbach, M., and Maney, T. (1999). Mutations in the ATP-binding domain affect the subcellular distribution of mitotic centromere-associated kinesin (MCAK). Cell Biol. Int. *23*, 275–286.
30. Hackney, D.D., Levitt, J.D., and Suhan, J. (1992). Kinesin undergoes a 9 S to 6 S conformational transition. J. Biol. Chem. *267*, 8696–8701.
31. Gennerich, A., and Vale, R.D. (2009). Walking the walk: how kinesin and dynein coordinate their steps. Curr. Opin. Cell Biol. *21*, 59–67.
32. Hertzer, K.M., and Walczak, C.E. (2008). The C-termini of tubulin and the specific geometry of tubulin substrates influence the depolymerization activity of MCAK. Cell Cycle *7*, 2727–2737.
33. Wagenbach, M., Domnitz, S., Wordeman, L., and Cooper, J. (2008). A kinesin-13 mutant catalytically depolymerizes microtubules in ADP. J. Cell Biol. *183*, 617–623.
34. Kline-Smith, S.L., Khodjakov, A., Hergert, P., and Walczak, C.E. (2004). Depletion of centromeric MCAK leads to chromosome congression and segregation defects due to improper kinetochore attachments. Mol. Biol. Cell *15*, 1146–1159.
35. Zhang, X., Lan, W., Ems-McClung, S.C., Stukenberg, P.T., and Walczak, C.E. (2007). Aurora B phosphorylates multiple sites on mitotic centromere-associated kinesin to spatially and temporally regulate its function. Mol. Biol. Cell *18*, 3264–3276.
36. Rizk, R.S., Bohannon, K., Wetzel, L., Powers, J.A., Shaw, S.L., and Walczak, C.E. (2009). MCAK and paclitaxel have differential effects on spindle microtubule organization and dynamics. Mol. Biol. Cell *20*, 1639–1651.
37. Wordeman, L., Wagenbach, M., and von Dassow, G. (2007). MCAK facilitates chromosome movement by promoting kinetochore microtubule turnover. J. Cell Biol. *179*, 869–879.
38. Cimini, D., Wan, X., Hirel, C.B., and Salmon, E.D. (2006). Aurora kinase promotes turnover of kinetochore microtubules to reduce chromosome segregation errors. Curr. Biol. *16*, 1711–1718.
39. Lampson, M.A., Renduchitala, K., Khodjakov, A., and Kapoor, T.M. (2004). Correcting improper chromosome-spindle attachments during cell division. Nat. Cell Biol. *6*, 232–237.
40. Cheeseman, I.M., Chappie, J.S., Wilson-Kubalek, E.M., and Desai, A. (2006). The conserved KMN network constitutes the core microtubule-binding site of the kinetochore. Cell *127*, 983–997.
41. DeLuca, J.G., Gall, W.E., Ciferri, C., Cimini, D., Musacchio, A., and Salmon, E.D. (2006). Kinetochore microtubule dynamics and attachment stability are regulated by Hec1. Cell *127*, 969–982.
42. Walczak, C.E., Gan, E.C., Desai, A., Mitchison, T.J., and Kline-Smith, S.L. (2002). The microtubule-destabilizing kinesin XKCM1 is required for chromosome positioning during spindle assembly. Curr. Biol. *12*, 1885–1889.